



Contents lists available at ScienceDirect

Spectrochimica Acta Part A: Molecular and Biomolecular Spectroscopy

journal homepage: www.elsevier.com/locate/saa

A vibrational spectroscopic study of the phosphate mineral minyulite $\text{KAl}_2(\text{OH},\text{F})(\text{PO}_4)_2 \cdot 4(\text{H}_2\text{O})$ and in comparison with wardite



Ray L. Frost^{a,*}, Andrés López^a, Yunfei Xi^a, Luiz Henrique Cardoso^b, Ricardo Scholz^b

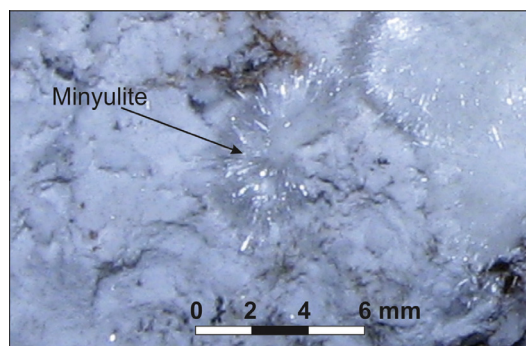
^a School of Chemistry, Physics and Mechanical Engineering, Science and Engineering Faculty, Queensland University of Technology, GPO Box 2434, Brisbane, Queensland 4001, Australia

^b Geology Department, School of Mines, Federal University of Ouro Preto, Campus Morro do Cruzeiro, Ouro Preto, MG 35,400-00, Brazil

HIGHLIGHTS

- We have studied the phosphate mineral minyulite Minyulo Well, Australia.
- We used vibrational spectroscopy to describe the vibrational modes of phosphate.
- A comparison is made with the spectra of the other phosphate mineral wardite.

GRAPHICAL ABSTRACT



ARTICLE INFO

Article history:

Received 1 October 2013

Received in revised form 2 December 2013

Accepted 4 December 2013

Available online 9 January 2014

Keywords:

Minyulite

Wardite

Phosphate

Hydroxyl

Raman spectroscopy

Infrared

ABSTRACT

Vibrational spectroscopy enables subtle details of the molecular structure of minyulite $\text{KAl}_2(\text{OH},\text{F})(\text{PO}_4)_2 \cdot 4(\text{H}_2\text{O})$. Single crystals of a pure phase from a Brazilian pegmatite were used. Minyulite belongs to the orthorhombic crystal system. This indicates that it has three axes of unequal length, yet all are perpendicular to each other. The infrared and Raman spectroscopy were applied to compare the structure of minyulite with wardite. The reason for the comparison is that both are Al containing phosphate minerals.

The Raman spectrum of minyulite shows an intense band at 1012 cm^{-1} assigned to the $\nu_1\text{ PO}_4^{3-}$ symmetric stretching vibrations. A series of low intensity Raman bands at $1047, 1077, 1091$ and 1105 cm^{-1} are assigned to the $\nu_3\text{ PO}_4^{3-}$ antisymmetric stretching modes. The Raman bands at $1136, 1155, 1176$ and 1190 cm^{-1} are assigned to AIOH deformation modes. The infrared band at 1014 cm^{-1} is ascribed to the $\text{PO}_4^{3-}\nu_1$ symmetric stretching vibrational mode. The infrared bands at $1049, 1071, 1091$ and 1123 cm^{-1} are attributed to the $\text{PO}_4^{3-}\nu_3$ antisymmetric stretching vibrations. The infrared bands at $1123, 1146$ and 1157 cm^{-1} are attributed to AIOH deformation modes. Raman bands at $575, 592, 606$ and 628 cm^{-1} are assigned to the ν_4 out of plane bending modes of the PO_4^{3-} unit. In the $2600\text{--}3800\text{ cm}^{-1}$ spectral range, Raman bands for minyulite are found at $3661, 3669$ and 3692 cm^{-1} are assigned to AIOH/AIF stretching vibrations. Broad infrared bands are also found at $2904, 3105, 3307, 3453$ and 3523 cm^{-1} . Raman bands at $3225, 3324\text{ cm}^{-1}$ are assigned to water stretching vibrations. A comparison is made with the vibrational spectra of wardite. Raman spectroscopy complimented with infrared spectroscopy has enabled aspects of the structure of minyulite to be ascertained and compared with that of other phosphate minerals.

© 2013 Elsevier B.V. All rights reserved.

* Corresponding author. Tel.: +61 7 3138 2407; fax: +61 7 3138 1804.

E-mail address: r.frost@qut.edu.au (R.L. Frost).

Introduction

Minyulite [1] is a rare phosphate mineral with a chemical formula of $KAl_2(OH,F)(PO_4)_2 \cdot 4(H_2O)$. It occurs as groups of radiating fine fibrous crystals within rock cracks of weathered glauconitic phosphatic ironstone [2]. It was first described in 1933 for an occurrence in Western Australia and named after the type locality Minyulo Well in Western Australia [1]. Minyulite is considered as a secondary phosphate since it is formed by the alteration of a primary phosphate [2]. Primary phosphates are phosphates that are mined on a large scale for example 'super phosphate' of calcium phosphate. The mineral minyulite occurs in association with other phosphate minerals including dufrenite, apatite, fluellite, wavellite, variscite and leucophosphate all of which are secondary phosphate minerals [3]. The mineral is known from many locations worldwide [4–7]. The mineral is found in many Australian localities including from near Minyulo Well, Dandarragan, Western Australia; in Wait's quarry and Oliver's quarry, near Noarlunga, 32 km south of Adelaide; in the Moculta phosphate quarry, northeast of Angaston, and from the St. John's quarry, seven km southeast of Kapunda, Mount Lofty Ranges, South Australia; at Wolfdene, near Beenleigh, Brisbane, Queensland. The mineral can be found in the underlying phosphatized rock zone of ornithogenic soil. Minyulite is not found in abundance, it can be found in the sea shore of the maritime Arctic and Antarctic [8,9]. The mineral minyulite is known from a wide range of deposits world-wide for example in Italy and in the USA. A comparison may be made with the mineral wardite $NaAl_3(PO_4)_2(OH)_4 \cdot 2(H_2O)$.

Minyulite belongs to the orthorhombic crystal system [10,11]. This indicates that it has three axes of unequal length, yet all are perpendicular to each other. The Space Group is *Pba*2. $a = 9.337(5)$ $b = 9.740(5)$ $c = 5.522(3)$ and $Z = 2$. The mineral wardite is unusual in that it belongs to a unique symmetry class, namely the tetragonal-trapezohedral group [12]. This class has only a 4-fold rotational axis and two 2-fold rotational axes and nothing else. Crystals of wardite show the lower symmetry by displaying squashed pseudo-octahedrons with striated faces.

The crystal structures of natural wardite and of the isomorphous cyrilovite have been solved [12,13]. The structure of cyrilovite was further refined by Cooper et al. The cell dimensions are *Space Group*: $P4_12_1$ or $P4_32_12$. $a = 7.03(1)$ Å, $c = 19.04(1)$ Å, $Z = 4$. The structures contain layers of two kinds of corner-linked —OH bridged MO_6 octahedra ($M = Al, Fe$), stacked along the tetragonal *C*-axis in a four-layer sequence and linked by PO_4 groups. Within a layer, e.g. around the (001) plane, two independent pairs of symmetry-correlated —OH groups are arranged in the equatorial pseudo-planes of one kind of MO_6 octahedra [12,13].

Raman spectroscopy has proven very useful for the study of minerals [14–20]. Indeed, Raman spectroscopy has proven most useful for the study of diagenetically related minerals where isomorphous substitution may occur as with wardite, cyrilovite and minyulite, as often occurs with minerals containing phosphate groups. This paper is a part of systematic studies of vibrational spectra of minerals of secondary origin. The objective of this research is to report the Raman and infrared spectra of minyulite and to relate the spectra to the molecular structure of the mineral.

Experimental

Samples description and preparation

The minyulite sample studied in this work was collected from Minyulo Well, Australia. The formula corresponds to $(K_{0.82}Ca_{0.05}Na_{0.03})(Al_{2.04}Fe_{0.08})(PO_4)_2[F_{0.55}(OH)_{0.45}] \cdot 4H_2O$. The sample was incorporated to the collection of the Geology Department of the

Federal University of Ouro Preto, Minas Gerais, Brazil, with sample code SAB-193. The sample was gently crushed and the associated minerals were removed under a stereomicroscope Leica MZ4. The minyulite sample was phase analyzed by X-ray diffraction. Scanning electron microscopy (SEM) in the EDS mode was applied to support the mineral characterization.

The mineral wardite was supplied by the Mineralogical Research Company. Wardite originated from Lavra Da Ilha, Minas Gerais, Brazil. Details of this mineral have been published (page 643) [21].

Raman spectroscopy

Crystals of minyulite were placed on a polished metal surface on the stage of an Olympus BHS microscope, which is equipped with 10 \times , 20 \times , and 50 \times objectives. The microscope is part of a Renishaw 1000 Raman microscope system, which also includes a monochromator, a filter system and a CCD detector (1024 pixels). The Raman spectra were excited by a Spectra-Physics model 127 He–Ne laser producing highly polarised light at 633 nm and collected at a nominal resolution of 2 cm^{-1} and a precision of ± 1 cm^{-1} in the range between 200 and 4000 cm^{-1} . Some of these mineral fluoresced badly at 633 nm; as a consequence other laser excitation wavelengths were used especially the 785 nm laser. Repeated acquisitions on the crystals using the highest magnification (50 \times) were accumulated to improve the signal to noise ratio of the spectra. Spectra were calibrated using the 520.5 cm^{-1} line of a silicon wafer. Previous studies by the authors provide more details of the experimental technique. Alignment of all crystals in a similar orientation has been attempted and achieved. However, differences in intensity may be observed due to minor differences in the crystal orientation.

Infrared spectroscopy

Infrared spectra were obtained using a Nicolet Nexus 870 FTIR spectrometer with a smart endurance single bounce diamond ATR cell. Spectra over the 4000–525 cm^{-1} range were obtained by the co-addition of 128 scans with a resolution of 4 cm^{-1} and a mirror velocity of 0.6329 cm/s. Spectra were co-added to improve the signal to noise ratio.

Spectral manipulation such as baseline correction/adjustment and smoothing were performed using the Spectralcalc software package GRAMS (Galactic Industries Corporation, NH, USA). Band component analysis was undertaken using the Jandel 'Peakfit' software package that enabled the type of fitting function to be selected and allows specific parameters to be fixed or varied accordingly. Band fitting was done using a Lorentzian–Gaussian cross-product function with the minimum number of component bands used for the fitting process. The Gaussian–Lorentzian ratio was maintained at values greater than 0.7 and fitting was undertaken until reproducible results were obtained with squared correlations of r^2 greater than 0.995.

Results and discussion

Vibrational spectroscopy background

In aqueous systems, the Raman spectra of phosphate oxyanions show a symmetric stretching mode (ν_1) at 938 cm^{-1} , an antisymmetric stretching mode (ν_3) at 1017 cm^{-1} , a symmetric bending mode (ν_2) at 420 cm^{-1} and a ν_4 bending mode at 567 cm^{-1} [22–24]. S.D. Ross in Farmer [25] listed some well-known minerals containing phosphate which were either hydrated or hydroxylated or both [25]. However not all phosphate minerals were listed and

there is a lack of information on anhydrous minerals. The vibrational spectrum of the dihydrogen phosphate anion has been reported by Farmer [25]. The PO_2 symmetric stretching mode occurs at 1072 cm^{-1} and the POH symmetric stretching mode at $\sim 878\text{ cm}^{-1}$. The POH antisymmetric stretching mode was found at 947 cm^{-1} and the $\text{P}(\text{OH})_2$ bending mode at 380 cm^{-1} . The band at 1150 cm^{-1} was assigned to the PO_2 antisymmetric stretching mode. The position of these bands will shift according to the crystal structure of the mineral.

The vibrational spectra of phosphate minerals have been published by Farmer's treatise Chapter 17 [25]. Table 17.III in Ref. [25] reports the band positions of a wide range of phosphates and arsenates, among other oxyanion minerals. The band positions for the monohydrogen phosphate anion of disodium hydrogen phosphate dihydrate is given as ν_1 at 820 and 866 cm^{-1} , ν_2 at around 460 cm^{-1} , ν_3 as 953 , 993 , 1055 , 1070 , 1120 and 1135 cm^{-1} , ν_4 at 520 , 539 , 558 , 575 cm^{-1} . The POH unit has vibrations associated with the OH specie. The stretching vibration of the POH units was tabulated as 2430 and 2870 cm^{-1} , and bending modes at 766 and 1256 cm^{-1} . Water stretching vibrations were found at 3050 and 3350 cm^{-1} . The position of the bands for the disodium hydrogen phosphate is very dependent on the waters of hydration. There have been several Raman spectroscopic studies of the monosodium dihydrogen phosphate chemicals [26–30].

Vibrational spectroscopy of the phosphate anion in minyulite

The Raman spectrum of minyulite in the $100\text{--}4000\text{ cm}^{-1}$ spectral range is illustrated in Fig. 1a. This Raman spectrum shows the position of the Raman bands and their relative intensities. It is obvious that there are large parts of the spectrum where little or no intensity is observed. Therefore, the spectrum is subdivided into

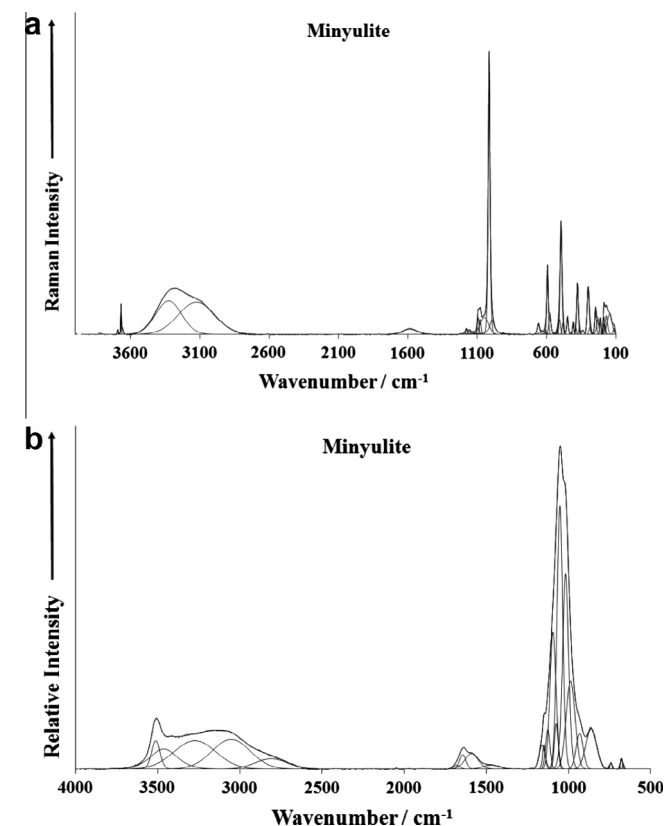


Fig. 1. (a) Raman spectrum of minyulite over the $100\text{--}4000\text{ cm}^{-1}$ spectral range and (b) infrared spectra of minyulite over the $500\text{--}4000\text{ cm}^{-1}$ spectral range.

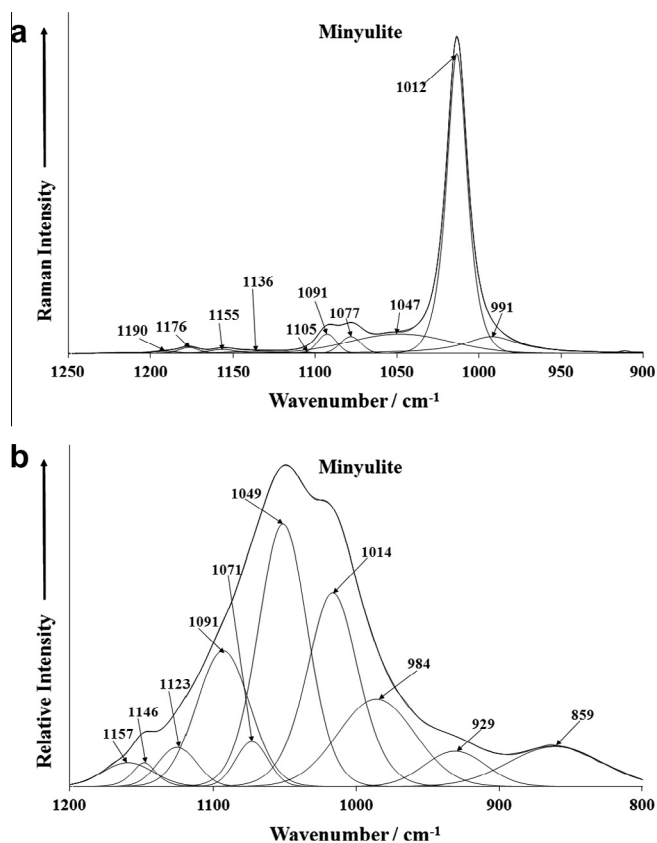


Fig. 2. (a) Raman spectrum of minyulite over the $900\text{--}1250\text{ cm}^{-1}$ range and (b) infrared spectrum of minyulite over the $800\text{--}1200\text{ cm}^{-1}$ range.

sections according to the type of vibration being investigated. In this way, the precise position of the bands can be detailed. The infrared spectrum of minyulite in the $500\text{--}4000\text{ cm}^{-1}$ spectral range is shown in Fig. 1b. The reflectance spectrum starts at $\sim 500\text{ cm}^{-1}$ because the ATR cell absorbs all infrared radiation below this wavenumber. As for the Raman spectrum, the infrared spectrum is subdivided into sections depending upon the type of vibration being examined. The complete infrared spectrum displays the position of the infrared bands and their relative intensity.

The Raman spectrum of minyulite over the $900\text{--}1250\text{ cm}^{-1}$ spectral range is illustrated in Fig. 2a. This spectral region is the region where the phosphate stretching modes are to be found. The spectrum is dominated by an intense broadish band at 1012 cm^{-1} . This band is assigned to the PO_4^{3-} ν_1 symmetric stretching vibration. A low intensity shoulder band on the low wavenumber side of this band at 991 cm^{-1} is also found. A series of low intensity Raman bands at 1047 , 1077 , 1091 , 1105 , 1136 , 1155 , 1176 and 1190 cm^{-1} . It is tempting to attribute these bands to PO_4^{3-} ν_3 antisymmetric stretching vibration. The first 4 or 5 bands are attributed to this vibration. The Raman bands at 1136 , 1155 , 1176 and 1190 cm^{-1} are assigned to ALOH deformation modes. The number of antisymmetric stretching modes provides evidence of reduced symmetry of the phosphate anion in the minyulite structure.

The Raman spectrum of wardite is dominated by two intense bands at around 995 and 1051 cm^{-1} . These two bands are assigned to the ν_1 PO_4^{3-} symmetric stretching vibrations. Two intense bands are observed reflecting two non-equivalent phosphate units in the wardite structure. Breitingner et al. [31] used FT-Raman to obtain their spectrum and found overlapping Raman bands at 999 and 1033 cm^{-1} and assigned these bands to the ν_1 PO_4^{3-} symmetric stretching and ν_3 PO_4^{3-} antisymmetric stretching modes. The

difference in the spectra between our work and that of Breitinger et al. [31], may be attributed to the improved technology of the spectrometer with greater resolution. Breitinger et al. also assigned the band at 999 cm^{-1} to AlOH deformation modes. In our work the Raman band at 995 cm^{-1} is very sharp and well resolved. The band at 1051 cm^{-1} is ever so slightly asymmetric on the low wavenumber side and a component may be resolved at 1045 cm^{-1} . A group of low intensity bands are observed at 1083, 1109, 1140 and 1186 cm^{-1} and are assigned to the $\nu_3\text{ PO}_4^{3-}$ antisymmetric stretching modes. Breitinger et al. did not report any bands in these positions in the Raman spectrum. These researchers reported infrared bands at 1058 (strong) with shoulders at 1129 and 1168 cm^{-1} and assigned these bands to $\delta\text{Al}_2\text{OH}$ deformation modes. A low intensity broad band at 884 cm^{-1} (a), 902 cm^{-1} (b) and 893 cm^{-1} (c) are assigned to a water librational mode. In the work of Breitinger et al. [31], a broad low intensity band was found at around 800 cm^{-1} and was attributed to water librational modes.

The infrared spectrum of minyulite over the $800\text{ to }1200\text{ cm}^{-1}$ spectral range is provided in Fig. 2b. The infrared spectrum is broad; however some spectral features are observed which may be resolved into component bands as is illustrated in this figure. The band at 1014 cm^{-1} is ascribed to the PO_4^{3-} ν_1 symmetric stretching vibrational mode. The infrared bands at 1049, 1071, 1091 and 1123 cm^{-1} are attributed to the PO_4^{3-} ν_3 antisymmetric stretching vibrations. The infrared bands at 1123, 1146 and 1157 cm^{-1} are ascribed to AlOH deformation modes. The infrared bands at 859, 929 and possibly the 984 cm^{-1} band are attributed to water librational modes. The infrared spectrum of wardite shows a great deal more complexity when compared with the Raman spectrum. The infrared band at around 994 cm^{-1} is attributed to the $\nu_1\text{ PO}_4^{3-}$ symmetric stretching mode. The cluster of bands at 1042, 1053, 1085, 1102, 1135 and 1165 cm^{-1} are attributed to the $\nu_3\text{ PO}_4^{3-}$ antisymmetric stretching modes. Some of these bands may

also be due to the $\delta\text{Al}_2\text{OH}$ deformation modes, in harmony with the assignment of Breitinger et al. Breitinger and co-workers stated that the deceptively simple strong IR band centered at 1059 cm^{-1} contains at least four components of $\nu(\text{PO}_4)$ generated by lifting of the originally threefold degeneracy of $\nu_3(\text{PO}_4)$ and activation of $\nu_1(\text{PO}_4)$ due to the general position of PO_4 and again at least four components of the deformation modes $\delta(\text{Al}_2\text{OH})$ involving the two pairs of the non-equivalent OH groups. In this work we have obtained much greater resolution and these components are resolved into the component bands.

The Raman spectrum of minyulite over the $400\text{--}700\text{ cm}^{-1}$ and $100\text{--}400\text{ cm}^{-1}$ spectral ranges are reported in Fig. 3. The spectrum in Fig. 3a may be subdivided into sections. (a) The bands at around 592 cm^{-1} , (b) the bands in the $448\text{--}535\text{ cm}^{-1}$ spectral range and (c) bands in the $350\text{--}400\text{ cm}^{-1}$. In addition, there is a low intensity band at 657 cm^{-1} . The Raman bands observed at 575, 592, 606 and 628 cm^{-1} are assigned to the ν_4 out of plane bending modes of the PO_4 and H_2PO_4 units. The Raman spectrum of NaH_2PO_4 shows bands at 526, 546 and 618 cm^{-1} (this work). The observation of multiple bands in this spectral region supports the concept of symmetry reduction of both the phosphate. Intense Raman bands of wardite are observed at 588 and 620 with an additional band at 559 cm^{-1} are assigned to the ν_4 out of plane bending modes of the PO_4^{3-} and HOPO_3^{2-} units. Breitinger et al. [31] assigned these bands to $\nu(\text{Al}(\text{O}/\text{OH})_6)$ stretching vibrations. No phosphate bending modes in the work of Breitinger et al. [31] were reported. The Raman spectrum of crystalline NaH_2PO_4 shows Raman bands at 526, 546 and 618 cm^{-1} (data obtained by the authors).

Raman bands observed at 407, 420, 448, 481, 494 and 506 cm^{-1} are attributed to the $\nu_2\text{ PO}_4$ and H_2PO_4 bending modes. The Raman spectrum of NaH_2PO_4 shows two Raman bands at 460 and 482 cm^{-1} . The observation of multiple Raman bands in this spectral region for the minyulite mineral supports the concept of symmetry reduction of the phosphate anion. A series of Raman bands for wardite are observed at 396, 416, 444, 464, and 489 cm^{-1} . These bands are attributed to the $\nu_2\text{ PO}_4^{3-}$ and H_2PO_4 bending modes. The Raman spectrum of NaH_2PO_4 shows Raman bands at 460 and 482 cm^{-1} . Thus, the series of Raman bands at 391, 401, 458, 485 and 510 cm^{-1} are attributed to the $\nu_2\text{ PO}_4^{3-}$ bending modes. Raman bands at 317, 446 and 515 cm^{-1} reported by Breitinger et al. were assigned to vibrational modes of the $\text{AlO}_6/\text{AlOH}_6$ units. In the infrared spectrum of wardite, a series of infrared bands are observed at 620, 643 and 673 cm^{-1} . These bands are attributed to the ν_4 out of plane bending modes of the PO_4^{3-} units. Breitinger et al. [31] assigned bands in this region to $\nu(\text{Al}(\text{O}/\text{OH})_6)$ stretching vibrations. In harmony with Breitinger et al. [31], assignments, the infrared bands observed at 732, 795 and 893 cm^{-1} are attributed to water librational modes. Infrared bands observed at 573, 578 and 587 cm^{-1} are attributed to $\gamma(\text{Al}_2\text{OH})$ vibrations.

Strong Raman bands are observed at 299, 338, 376 and 388 cm^{-1} with shoulder bands at 285, 362, and 388 cm^{-1} . These bands are assigned to metal–oxygen stretching vibrations. Again, the observation of multiple bands in this spectral region supports the concept of the non-equivalence of MO units in the structure of minyulite. There are a number of bands in the Raman spectrum of the far low wavenumber region (Fig. 5b). These bands are ascribed to lattice vibrations. Intense Raman bands for wardite observed at 258 cm^{-1} and 299 cm^{-1} are related to the O–Al–O skeletal stretching vibrations. The intense band in all the spectra at 177 cm^{-1} is considered to be associated with H–OH hydrogen bonds.

The Raman spectrum of minyulite over the $2800\text{--}3800\text{ cm}^{-1}$ spectral range is given in Fig. 4a. The infrared spectrum of minyulite over the $2500\text{--}3800\text{ cm}^{-1}$ spectral range is given in Fig. 4b. There are two features of the Raman spectrum in this spectral region: (a) the very broad feature centred upon around

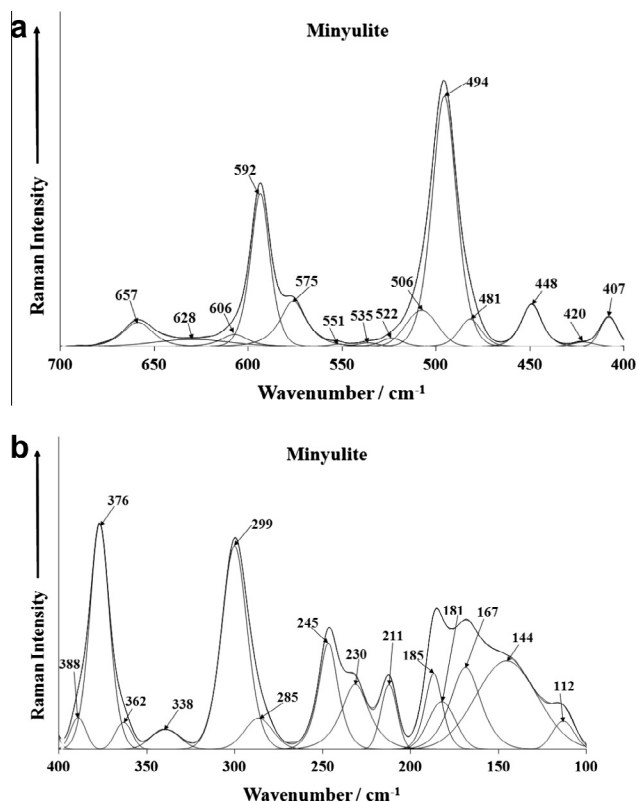


Fig. 3. (a) Raman spectrum of minyulite over the $400\text{--}700\text{ cm}^{-1}$ range and (b) Raman spectrum of minyulite over the $100\text{--}400\text{ cm}^{-1}$ range.

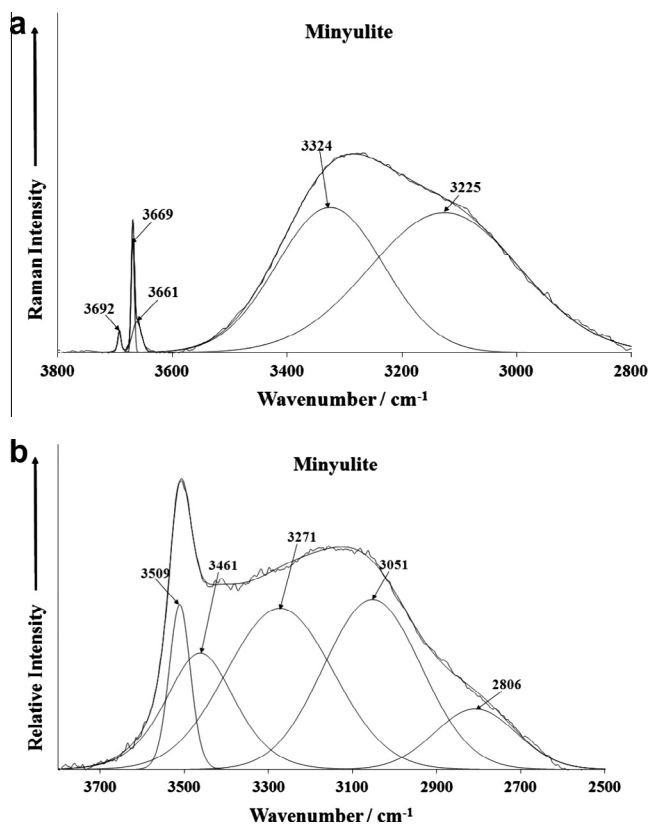


Fig. 4. (a) Raman spectrum of minyulite over the 2800–3800 cm⁻¹ spectral range and (b) infrared spectrum of minyulite over the 2500–3800 cm⁻¹ range.

3324 cm⁻¹ and (b) the very sharp bands at around 3669 cm⁻¹. The three bands at 3661, 3669 and 3692 cm⁻¹ are assigned to AlOH stretching vibrations. The broad feature may be resolved into component bands at 3225, 3324 cm⁻¹ and these bands are assigned to water stretching vibrations. The Raman band which is assigned to AlF vibrations is found between 800 and 1000 cm⁻¹.

The infrared spectrum shows sharpish band at 3509 cm⁻¹ which may be assigned to the OH stretching vibrations. As with the Raman spectrum, the broad feature centred around 3200 cm⁻¹ may be resolved into component bands at 2806, 3051, 3271 and 3461 cm⁻¹. These bands are assigned to water stretching vibrations. The infrared spectrum of wardite mineral samples display infrared bands at 3545 and 3611 cm⁻¹ and are attributed to the OH stretching vibrations of the hydroxyl units. Two shoulder bands are observed at 3532 and 3601 cm⁻¹ are also assigned to the OH stretching vibrations. A sharp band in the infrared spectrum is observed at 3480 cm⁻¹ for some wardite samples. This band may be due to FeOH stretching vibrations. Breitingner et al. [31] found infrared bands at 3520 (vw), 3545 (s), 3585 (sh) and 3613 cm⁻¹ (m). Breitingner et al. states that the $\nu(\text{OH})$ modes in the two independent pairs of symmetry-correlated OH groups classify as 2a + 2b; with the correlation splitting between a and b species depending on the distances in each of the pairs [31]. The $\nu(\text{OH})$ region of IR spectra of wardite shows two sharp bands (3613 and 3545 cm⁻¹) with two weak shoulders or satellites (3580 and 3520 cm⁻¹). It is likely that the two sharp infrared bands are due to two independent and non-equivalent OH units. The two sharp shoulder bands may be attributed to the Al–OH–Fe groups, i.e. the cyrilovite part of the solid solution. Broad infrared bands for wardite are observed at 2876 and 3266 cm⁻¹. These bands are assigned to water stretching vibrations. It is probable that some of the component bands are due to overtones and combination of

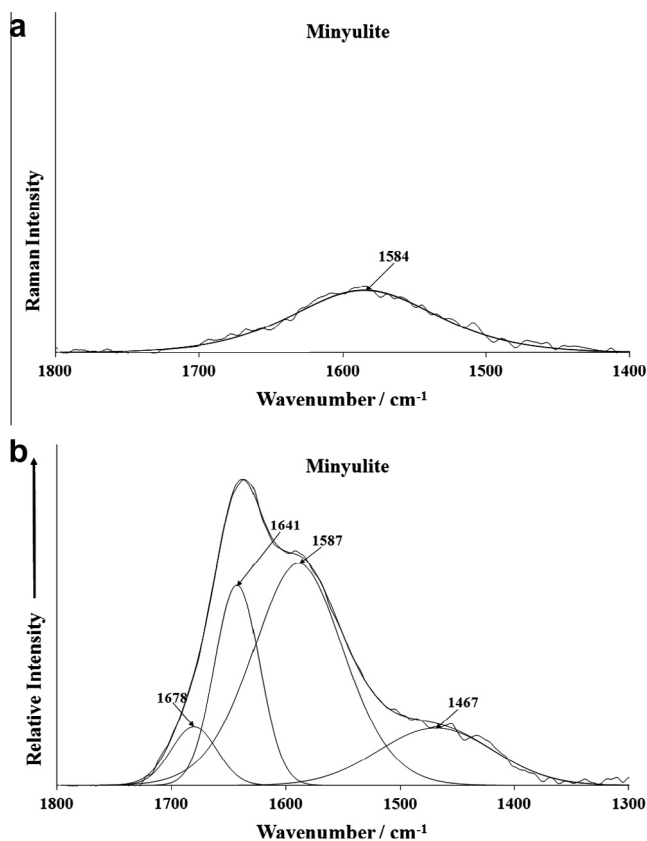


Fig. 5. (a) Raman spectrum of minyulite over the 1400–1800 cm⁻¹ spectral range and (b) infrared spectrum of minyulite over the 1300–1800 cm⁻¹ range.

the water bending and librational modes. The position of the water stretching vibration provides evidence for strong hydrogen bonding and that water is involved in different hydrogen bonding arrangements. The band at around 2876 cm⁻¹ gives an indication that water is very strongly hydrogen bonded in the wardite structure.

The Raman spectrum of minyulite in the 1400–1800 cm⁻¹ spectral range is reported in Fig. 5a. The infrared spectrum of minyulite in the 1300–1800 cm⁻¹ spectral range is reported in Fig. 5b. The Raman spectrum displays a low intensity Raman band at 1584 cm⁻¹ which is assigned to the water bending mode. This band is also observed in the infrared spectrum at 1587 cm⁻¹. This band is indicative of very weakly hydrogen bonded water. The infrared band at 1641 cm⁻¹ which is not observed in the Raman spectrum is attributed to more strongly hydrogen bonded water. The infrared band at 1467 cm⁻¹ may be an overtone or combination band.

Conclusions

Minyulite is a hydrated hydroxyl phosphate of potassium and aluminium $\text{KAl}_2(\text{OH},\text{F})(\text{PO}_4)_2 \cdot 4(\text{H}_2\text{O})$. The mineral is structurally and chemically related to wardite.

Raman spectroscopy complimented with infrared spectroscopy has been used to study aspects of the molecular structure of the mineral minyulite. The structure of minyulite is orthorhombic. As a consequence multiple phosphate vibrational modes are observed. Raman and infrared bands are observed and attributed to phosphate, hydroxyl and water vibrational stretching and bending modes. The structure of wardite contains layers of corner-linked –OH bridged MO_6 octahedra stacked along the tetragonal C-axis

in a four-layer sequence and linked by PO₄ groups. As a consequence at the molecular level non-equivalent phosphate units exist in the structure. As a consequence multiple phosphate vibrational modes are observed.

Acknowledgments

The financial and infra-structure support of the Queensland University of Technology, Chemistry discipline is gratefully acknowledged. The Australian Research Council (ARC) is thanked for funding the instrumentation. The authors would like to acknowledge the Center of Microscopy at the Universidade Federal de Minas Gerais (<http://www.microscopia.ufmg.br>) for providing the equipment and technical support for experiments involving electron microscopy. R. Scholz thanks to CNPq – Conselho Nacional de Desenvolvimento Científico e Tecnológico (Grant Nos. 306287/2012-9 and 402852/2012-5).

References

- [1] E.S. Simpson, C.R. LeMesurier, *J. Roy. Soc. W. Aust.* **19** (1933) 13–16.
- [2] L.J. Spencer, F.A. Bannister, M.H. Hey, H. Bennett, *Mineral. Mag.* **26** (1943) 309–314.
- [3] E.R. Segnit, J. Watts, *Mater. S'ezda MMA*, 11th, (1981) 273–279.
- [4] R. van Tassel, *Bull. Inst. Roy. Sci. Nat. Belg.* **36** (1960) 1–4.
- [5] A.M. Fransolet, J. Jedwab, R. Van Tassel, *Ann. Soc. Geol. Belg.* **97** (1975) 331–340.
- [6] S. Menchetti, C. Sabelli, *Neues Jahrb. Mineral. Mt.* (1981) 505–510.
- [7] E.A. Ankinovich, I.S. Zazubina, *Petrol. i Petrokhimiya Magmat. i Metamorf. Porod Kazakhstana i Mestorozhd., s nimi Svyaz.*, Alma-Ata, (1987) 22–28.
- [8] A. Tatur, A. Barczuk, *Antarct. Nutr. Cycles food webs*, in: SCAR Symp. Antarct. Biol., 4th, 1985, pp. 163–168.
- [9] F.N.B. Simas, C.E.G.R. Schaefer, V.F. Melo, M.R. Albuquerque-Filho, R.F.M. Michel, V.V. Pereira, M.R.M. Gomes, L.M. da Costa, *Geoderma* **138** (2007) 191–203.
- [10] A.R. Kampf, *Am. Mineral.* **62** (1977) 256–262.
- [11] F.C. Hawthorne, *Zeit. Krist.* **192** (1990) 1–52.
- [12] L. Fanfani, A. Nunzi, P.F. Zanazzi, *Mineral. Mag.* **37** (1970) 598–605.
- [13] D. Cozzupoli, O. Grubessi, A. Mottana, P.F. Zanazzi, *Mineral. Petrol.* **37** (1987) 1–14.
- [14] R.L. Frost, Y. Xi, R. Scholz, M. Belotti Fernanda, *Spectrochim. Acta A103* (2013) 143–150.
- [15] R.L. Frost, Y. Xi, R. Scholz, M. Belotti Fernanda, A. Dias Menezes Filho Luiz, *Spectrochim. Acta A 104* (2013) 250–256.
- [16] R.L. Frost, A. Lopez, Y. Xi, A. Granja, R. Scholz, R.M.F. Lima, *Spectrochim. Acta A114* (2013) 309–315.
- [17] R.L. Frost, Y. Xi, M. Beganovic, F.M. Belotti, R. Scholz, *Spectrochim. Acta A107* (2013) 241–247.
- [18] R.L. Frost, Y. Xi, R. Scholz, *Spectrochim. Acta A108* (2013) 244–250.
- [19] R.L. Frost, Y. Xi, R. Scholz, F.M. Belotti, *Spectrochim. Acta A105* (2013) 359–364.
- [20] R.L. Frost, Y. Xi, R. Scholz, F.M. Belotti, M. Beganovic, *Spectrochim. Acta A110* (2013) 7–13.
- [21] J.W. Anthony, R.A. Bideaux, K.W. Bladh, M.C. Nichols, *Handbook of Mineralogy, Mineral Data Publishing, Tuscon, Arizona, USA*, 1995.
- [22] R.L. Frost, W. Martens, P.A. Williams, J.T. Kloprogge, *Mineral. Mag.* **66** (2002) 1063–1073.
- [23] R.L. Frost, W.N. Martens, T. Kloprogge, P.A. Williams, *Neues Jahrb. Mineral. Mt.* (2002) 481–496.
- [24] R.L. Frost, P.A. Williams, W. Martens, J.T. Kloprogge, P. Leverett, *J. Raman Spectrosc.* **33** (2002) 260–263.
- [25] V.C. Farmer, *Mineralogical Society Monograph 4: The Infrared Spectra of Minerals*, London, 1974.
- [26] C.E. Bamberger, W.R. Busing, G.M. Begun, R.G. Haire, L.C. Ellingboe, *J. Solid State Chem.* **57** (1985) 248–259.
- [27] B.K. Choi, M.N. Lee, J.J. Kim, *J. Raman Spectrosc.* **20** (1989) 11–15.
- [28] A. Galy, *J. Phys. Rad.* **12** (1951) 827.
- [29] H. Poulet, N. Toupry-Krauzman, in: *Proc. Int. Conf. Raman Spectrosc.* 6th, vol. 2, 1978, pp. 364–365.
- [30] N. Toupry-Krauzman, H. Poulet, M. Le Postollec, *J. Raman Spectrosc.* **8** (1979) 115–121.
- [31] D.K. Breiting, H.H. Belz, L. Hajba, V. Komlosi, J. Mink, G. Brehm, D. Colognesi, S.F. Parker, R.G. Schwab, *J. Mol. Struct.* **706** (2004) 95–99.